Theor. Appl. Climatol. 89, 9–24 (2007)
DOI 10.1007/s00704-006-0260-6
Printed in The Netherlands

Theoretical and Applied Climatology

A. M. Obukhov Institute of Atmospheric Physics RAS, Moscow, Russia

Carbon cycle–climate feedback sensitivity to parameter changes of a zero-dimensional terrestrial carbon cycle scheme in a climate model of intermediate complexity

A. V. Eliseev and **I. I. Mokhov**

With 6 Figures

Received December 13, 2005; revised April 18, 2006; accepted June 5, 2006
Published online October 25, 2006

Summary

A series of sensitivity runs have been performed with a coupled climate–carbon cycle model. The climatic component consists of the climate model of intermediate complexity IAP RAS CM. The carbon cycle component is formulated as a simple zero-dimensional model. Its terrestrial part includes gross photosynthesis, and plant and soil respirations, depending on temperature via Q_{10}-relationships (Lenton, 2000). Oceanic uptake of anthropogenic carbon is formulated is a bi-linear function of tendencies of atmospheric concentration of CO_2 and globally averaged annual mean sea surface temperature. The model is forced by the historical industrial and land use emissions of carbon dioxide for the second half of the 19th and the whole of the 20th centuries, and by the emission scenario SRES A2 for the 21st century. For the standard set of the governing parameters, the model realistically captures the main features of the Earth's observed carbon cycle. A large number of simulations have been performed, perturbing the governing parameters of the terrestrial carbon cycle model. In addition, the climate part is perturbed, either by zeroing or artificially increasing the climate model sensitivity to the doubling of the atmospheric CO_2 concentration. Performing the above mentioned perturbations, it is possible to mimic most of the range found in the C4MIP simulations. In this way, a wide range of the climate–carbon cycle feedback strengths is obtained, differing even in the sign of the feedback. If the performed simulations are subjected to the constraints of a maximum allowed deviation of the simulated atmospheric CO_2 concentration ($pCO_{2(a)}$) from the observed values and correspondence between simulated and observed terrestrial uptakes, it is possible to narrow the corresponding uncertainty range. Among these constraints, considering $pCO_{2(a)}$ and uptakes are both important. However, the terrestrial uptakes constrain the simulations more effectively than the oceanic ones. These constraints, while useful, are still unable to rule out both extremely strong positive and modest negative climate–carbon cycle feedback.

1. Introduction

Beginning with the paper by Cox et al. (2000), the majority of climate modelling efforts have been devoted to the simulation of the global carbon cycle, interactively coupled with three-dimensional climate models (Brovkin et al., 2002, 2004; Friedlingstein et al., 2001, 2003; Dufresne et al., 2002; Jones et al., 2003; Matthews et al., 2004, 2005). These papers have shown that this interactive coupling changes the build up of carbon dioxide in the atmosphere $pCO_{2(a)}$ in comparison with the hypothetical case, when the carbon cycle is not affected by changes in the climate. As a result, the so called climate–carbon cycle feedback has been introduced. This feedback can be measured, for instance, as the difference in the atmospheric CO_2 concentration at some pre-chosen year under a specific carbon dioxide emission

scenario between two sets of numerical experiments. In the first set, the coupled simulation is performed with the climate–carbon cycle model, forced by CO_2 emissions. In the second set (uncoupled simulation), the climate model is forced by the output of the carbon cycle model; in turn, the carbon cycle model is forced by the CO_2 emissions, but does not take into account the influence of climate changes on carbon cycle dynamics. The climate–carbon cycle feedback can be measured either in terms of the feedback parameter f, or in terms of the feedback gain g (Friedlingstein et al., 2001). The feedback parameter is the change in atmospheric carbon dioxide concentration in a coupled simulation, divided by the corresponding concentration change in an uncoupled simulation. The gain is simply $g = f/(f-1)$.

To date, all coupled models simulate a positive climate–carbon cycle feedback, i.e., an interactive coupling between the climate and the carbon cycle increases the build up of carbon dioxide in the atmosphere (Cox et al., 2000; Friedlingstein et al., 2001; Brovkin et al., 2002, 2004; Dufresne et al., 2002; Jones et al., 2003; Matthews et al., 2004, 2005). However, the simulated intensity of the carbon cycle falls into a rather broad range. For instance, Cox et al. (2000) estimated this additional build up as amounting to 250 ppmv, while Dufresne et al. (2002) obtained a value of 75 ppmv. This discrepancy has led to the intercomparison of coupled climate–carbon cycle models. Suitable techniques for such intercomparison have been developed in Friedlingstein et al. (2003). The most comprehensive intercomparison has been performed in the framework of the Coupled Climate–Carbon Cycle Models Intercomparison Project (C4MIP) (Friedlingstein et al., 2006), which compares models of differing complexity, forced by the same emission scenario.

However, this intercomparison has yielded a wider range of characteristics for the coupled climate–carbon cycle simulations. Different formulations of the climate and carbon cycle components have resulted in notable differences between the model simulations.

Moreover, even the sign of the climate–carbon cycle feedback can be questioned. The positive feedback found in the simulations is basically associated with enhanced soil respiration in warmer climates (and to a smaller extent, to enhanced plant respiration). This effect overwhelms the direct fertilisation effect of carbon dioxide. However, Melillo et al. (2002), based on the direct results of the field measurements, noted that the nitrogen limitation of organic matter decomposition in soils may lead to the final decrease of soil respiration under increasing temperatures. Moreover, the response of gross plant photosynthesis to climate changes is ambigious. Starting from the present day climate, warmer temperatures and increased precipitation have generally led to enhanced plant photosynthesis (Adams et al., 2004; Huntingford et al., 2000). However, further climate changes may decrease this photosynthesis due to, e.g. the dieback of living biota (Adams et al., 2004; Huntingford et al., 2000). Furthermore, this effect can be regionally dependent; in particular, strong dieback of the Amazonian forests can be expected (Cox et al., 2004; Huntingford et al., 2004). Even the traditional approach of quantifying the temperature dependence of soil respiration, the Q_{10} factor (the value which serves as a multiplier for the soil respiration value, if temperature is increased by 10 °C), varies over a rather broad range. Raich and Schlesinger (1992) and Lloyd and Taylor (1994), based on extensive reviews of earlier studies for particular soil samples, suggested the corresponding range $Q_{10,s} = 1.3 - 3.3$. A similar, but narrower range 1.4–2.8 has been obtained by Jones and Cox (2001), based on the large scale/long term observational estimations of soil respiration variability. The uppermost value for $Q_{10,s}$ has been obtained by Trumbore et al. (1996), based on the fast cycling fraction of soil. Combined with the uncertainties in other governing parameters (see below), this uncertainty inevitably brings considerable spread to the results of the simulated climate–carbon cycle feedback.

The goal of the present paper is to examine the possible range of the climate–carbon cycle feedback, using a simple, but flexible, carbon cycle model, coupled to the climate model of intermediate complexity IAP RAS CM (Mokhov et al., 2006; Eliseev et al., 2006). Its terrestrial component stems from the model by Lenton (2000) with gross photosynthesis, and plant and soil respiration, depending on temperature via Q_{10}-relationships. Oceanic uptake of anthropogenic carbon is formulated as a bi-linear function of tendencies of atmospheric concentration of CO_2,

and globally averaged annual mean sea surface temperature. In this paper, the terrestrial carbon cycle is perturbed, varying its governing parameters, based on the published ranges of their values. The climate part of the model is perturbed by artificial increase or decrease of model sensitivity to atmospheric CO_2 content. To distinguish between realistic and unrealistic situations, the simulations are subjected to the constraint of the proximity to the observed carbon cycle characteristics. The latter constraint has not been imposed in the analyses published by C4MIP.

Other than the above mentioned sources of simulation uncertainty, e.g. forcings due to aerosols, anthropogenic greenhouse gases due to other than CO_2, solar and volcanic activity and emissions (especially from land-use), and missing model processes (such as nitrogen cycling, fire activity or atmospheric chemistry) are not considered in this paper.

2. Description of the model

2.1 Climate model

The climate model of intermediate complexity, developed at the A. M. Obukhov Institute of Atmospheric Physics RAS (IAP RAS CM), has been comprehensively described in previous literature (Petoukhov et al., 1998; Handorf et al., 1999; Mokhov et al., 2002, 2005). It employs modules for the redistribution of shortwave and longwave radiation, convection, cloud and precipitation formation. Large-scale atmospheric and oceanic dynamics (with scales larger than those corresponding to synoptic processes) are resolved explicitly. The synoptic-scale processes are treated as Gaussian ensembles. Sea ice in IAP RAS CM is diagnosed based on surface air and sea surface temperatures. In the model version used here, surface hydrology is prescribed. The IAP RAS CM horizontal resolution is 4.5 degrees latitude and 6.0 degrees longitude with 8 vertical layers in the atmosphere (up to 80 km) and 4 layers in the ocean. The quality of the IAP RAS CM's simulation of present-day climate is discussed in Mokhov et al. (2002, 2005) and Petoukhov et al. (2005). The sensitivity of this model to the doubling the carbon dioxide in the atmosphere is 2.2 °C and lies in the middle range of the current generation of the climate models (Mokhov et al., 2005; Petoukhov et al., 2005).

For the purposes of the present paper, IAP RAS CM (Mokhov et al., 2005) has been extended by the zero-dimensional carbon cycle model (Mokhov et al., 2006), which is described below.

2.2 Carbon cycle model

2.2.1 Carbon budget of the atmosphere

Annual mean budget of carbon dioxide in the atmosphere can be formulated for the atmospheric CO_2 concentration $p\mathrm{CO}_{2(a)}$:

$$\frac{dp\mathrm{CO}_{2(a)}}{dt} = E_f + D - F_l - F_{oc}, \tag{1}$$

where t is time, E_f and D are carbon dioxide emissions due to fossil fuel burning and industry, and land use, respectively (household emissions are neglected), F_l and F_{oc} represent CO_2 uptake by the land vegetation-soil system and by the world ocean, respectively.

2.2.2 Terrestrial carbon compartments

Carbon uptake by the terrestrial vegetation-soil system is modelled based on zero-dimensional equations (Svirezhev et al., 1985; Kwon and Schnoor, 1994; Lenton, 2000)

$$\begin{aligned} \frac{dC_v}{dt} &= NPP - L - D, \\ \frac{dC_s}{dt} &= L - R_s, \end{aligned} \tag{2}$$

where C_v and C_s are carbon terrestrial vegetation and soil stocks, NPP is the terrestrial vegetation net primary productivity, L is litterfall, R_s is heterotrophic (soil) respiration. The terms on the right hand sides of Eq. (2) depend on the corresponding carbon stocks and on the $\Delta T_{s,g}$ anomaly of globally averaged annual mean surface air temperature (GSAT) from the reference value (which will be specified later) (Lenton, 2000)

$$\begin{aligned} NPP &= P - R_p, \\ P &= A_p g_f(p\mathrm{CO}_{2(a)}) C_{v(s)} Q_{10,p}^{\Delta T_{s,g}/\Delta T_0} \\ R_p &= A_r C_v Q_{10,r}^{\Delta T_{s,g}/\Delta T_0}, \\ L &= A_l C_v, \\ R_s &= A_s C_s Q_{10,s}^{\Delta T_{s,g}/\Delta T_0}. \end{aligned} \tag{3}$$

Here, P is carbon production rate of photosynthesis, R_p is autotrophic (biota) respiration rate and A_p, A_r, A_l, A_s are constants. The temperature dependencies of the carbon fluxes are formulated in the most simplistic way, being proportional to $Q_{10,x}^{\Delta T_{s,g}/\Delta T_0}$, where $\Delta T_0 = 10\,\mathrm{K}$, $Q_{10,x}$ are constants, $x = p, r, s$ (Lloyd and Taylor, 1994). While this approach performs unsatisfactorily for the model employing regional and/or seasonal resolution (Lloyd and Taylor, 1994), it is considered to describe the climate dependencies of the globally averaged annual mean carbon fluxes (Raich and Schlesinger, 1992; Lenton, 2000) quite realistically. The reason for this is due to the relatively small $\Delta T_{s,g}$ under climate change, which is expected in this century, in comparison to the regional and seasonal variations of the surface air temperature. On the other hand, its simple formulation, employing only a few parameters, makes it attractive to consider the parametric sensitivity of the carbon cycle model under broad variations of those parameters. In principle, it is possible to expect that the litterfall intensity would vary with temperature as well, e.g. due to the dieback effect. However, this is not considered here. In Eq. (3) g_f is the fertility factor, which is formulated in accordance to the Michaelis-Menten law (see, e.g. Lenton, 2000)

$$g_f(p\mathrm{CO}_{2(a)}) = \begin{cases} 0 & \text{for } p\mathrm{CO}_{2(a)} < k_c, \\ \frac{p\mathrm{CO}_{2(a)} - k_c}{k_M + p\mathrm{CO}_{2(a)} - k_c} & \text{otherwise}, \end{cases}$$

where k_M is the half-saturation point, k_c is the compensation point (the threshold concentration of carbon dioxide in the atmosphere needed to initiate photosynthesis). $C_{v(s)}$ is the steady state living biomass, corrected for agriculture harvesting. This variable is modelled using the additional prognostic equation (Lenton, 2000):

$$\frac{dC_{v(s)}}{dt} = -k_D D, \tag{4}$$

k_D is constant. In the absence of land use emissions, total mass of carbon, stored in the living biomass would remain unchanged in this particular model. In the presence of positive land use emissions, it would decrease. To prevent it becoming negative, $C_{v(s)}$ is constrained to remain unchanged if it crosses zero. However, as a result of the relative (in comparison to its initial value, see below) smallness of the land use emissions used in the present paper, $C_{v(s)}$ does not cross zero. Carbon runoff to the ocean is neglected, because its contribution is small, 0.5–1.0 GtC/yr (Houghton et al., 1992). Finally, by carbon uptake by the terrestrial vegetation-soil system is represented by

$$F_l = NPP - R_s. \tag{5}$$

Compared to previous studies utilizing zero-dimensional terrestrial carbon cycle models, the model used here is most similar to that originally developed by Lenton (2000). However, it is not identical due to different temperature relationships of the biota photosynthesis and the biota and soil respirations. The cubic polynome, used originally by Lenton (2000), increases in the temperature range 0–27 °C, and declines afterwards, reaching zero at 40 °C (Lenton, 2000; Adams et al., 2004). The $T_{s,g}$, predicted by IAP RAS CM during the course of the SRES emissions is hardly expected to leave the growing part of this curve. As a result, in the model used here, this cubic polynome is replaced by the Q_{10}-relationship. A more subtle difference is due to the reference temperature value from which the GSAT anomalies are computed. In the Lenton (2000) model, this reference temperature is prescribed to be 288.15 K. In the present paper, both climate and carbon cycle are equilibrated for the pre-industrial state (see below) which is colder.

There is considerable uncertainty in the choice of the above mentioned above Q_{10}'s. Lenton (2000), based on a literature review, suggests the following ranges: $Q_{10,p} = 1.1-2.66$, $Q_{10,r} = 1.4-3.0$, $Q_{10,s} = 1.3-3.8$ with the "best guesses" 1.5, 2.15, 2.4, respectively. Jones and Cox (2001) estimate the range for $Q_{10,s} = 1.4-2.8$, based on climate variations due to El Niño events and volcanic activity, and adopt the value 2.0 for the Hadley Centre general circulation model. Here, Lenton's "best guess" values are adopted for the standard implementation of the zero-dimensional carbon cycle model.

For constants k_M and k_c, the values 150 and 29 ppmv are applied, respectively (Lenton, 2000). The value of k_M is considerably smaller than the usually adopted values of 400–460 ppmv (Farquhar et al., 1980; Budyko and Izrael, 1991). This choice is dictated by the peculiar formulation of gross photosynthesis, adopted in Lenton (2000). In the latter model, gross photosynthesis does not depend on the vegetation carbon stock

(Adams et al., 2004). This feature has to be compensated by a flatter fertilisation curve, corresponding to the smaller values of k_M. For the constant k_D, the value 0.27 is assigned (Lenton, 2000).

The values of other model parameters are tuned to simulate the pre-industrial carbon cycle state, which is assumed to be in equilibrium (Svirezhev et al., 1985) with $pCO_{2(a),0} = 280.0$ ppmv, $C_{s,0} = 1.5\times10^{15}$ kgC, $C_{v,0} = 0.55\times10^{15}$ kgC, $C_{v(s),0} = 0.55\times10^{15}$ kgC, $R_{p,0} = 5\times10^{13}$ kgC/yr, $L_0 = 5\times10^{13}$ kgC/yr (Houghton et al., 1992). As a result, the adopted values correspond to the time scales $A_l^{-1} = A_r^{-1} = 11$ yr, $A_s^{-1} = (A_l C_{lb,0}/C_{s,0})^{-1} = 30$ yr, $A_p^{-1} = (A_l + A_r)/g_f(pCO_{2(a),0}) = 3.4$ yr. Correspondingly, $\Delta T_{s,g}$ in the model is defined as an anomaly from the equilibrated pre-industrial GSAT.

2.2.3 Carbon uptake by the ocean

It is broadly accepted that the ocean exchanges inorganic carbon with the atmosphere, based simply on the solubility of carbon in sea water, while oceanic chemistry can be treated as a background process (Siegenthaler and Sarmiento, 1993). The oceanic solubility of carbon depends on the difference between the partial pressures of carbon dioxide in the atmosphere and in the ocean. Moreover, the passive role of oceanic chemistry allows one to relate the partial pressure of carbon dioxide in the upper layer of the ocean to sea surface temperature (SST) and to the three-dimensional oceanic circulation. On the global scale, SST can be used as a proxy for oceanic circulation. As a result, it is possible to relate carbon uptake by the ocean to the globally averaged annual mean SST $T_{oc,g}$, and to the atmospheric concentration of carbon dioxide $pCO_{2(a)}$. Here, the linear form of this dependence is employed (Thomas et al., 2001; Friedlingstein et al., 2003):

$$F_{as} = u_c \frac{dpCO_{2(a)}}{dt} - u_T \frac{dT_{oc,g}}{dt}. \qquad (6)$$

The values u_c and u_T are tuned to reproduce the observational based estimations of oceanic carbon uptake during the 1980s and 1990s (Houghton et al., 2001; Plattner et al., 2002; House et al., 2003; Le Quéré et al., 2003), given the observed trends of GSAT (Jones et al., 1999) and the atmospheric concentration of carbon dioxide Keeling et al., 1996) for the 20th century. As a result, the chosen values of the coefficients in Eq. (6) are $u_c = 1.31\times10^{12}$ kg/ppmv, $u_T = 0.33\times10^{14}$ kg/K.

Formulation of F_{as} in (6) possesses a physically desirable feature to be zero in an equilibrium state. However, it could behave incorrectly if emissions stop abruptly (E.M. Volodin, pers. comm.; it was also pointed out by one of the anonymous referees). After such emission stop, in reality $pCO_{2(a)}$ is expected to decrease due to continuing ocean uptake. In the model used here, it would start to increase, because the ocean would start to outgas CO_2. As a result, Eq. (6) is expected to be realistic only under continuing emissions of CO_2 and cannot be used in other circumstances.

3. Design of the numerical experiments

Three sets of model simulations were performed. These sets differ with respect to the climate–carbon cycle interactions.

In the first set (hereafter denoted as ''REF''), the interactively coupled climate–carbon cycle model is run. The coupled model is forced by CO_2 emissions. For 1860–2000, fossil fuel and industrial emissions and land use emissions are prescribed according to the data (Marland et al., 2005; Houghton, 2003). For 2000–2100, scenarios for both emissions are taken from the SRES emission scenario A2 (Houghton et al., 2001). The combined historical + SRES A2 scenario is similar to that used in the relatively recent works on the topic of climate–carbon cycle feedback (Brovkin et al., 2002, 2004, Dufresne et al., 2002; Friedlingstein et al., 2003; Jones et al., 2003; Matthews et al., 2004, 2005). The cumulative (industrial + land use) emissions during 1860–2100 amount to about 2.2×10^3 GtC.

In the second scenario group (denoted as ''NOCLIM''), the climate model is forced by the output of the carbon cycle model; in turn, the carbon cycle model is forced by CO_2 emissions, but the carbon cycle dynamics are not affected by the corresponding climate changes (due to zeroing of $\Delta T_{s,g}$ and $\Delta T_{oc,g}$, entering the carbon cycle routine).

The intensity of the carbon cycle feedback may depend on the overall sensitivity of the climate model to the carbon dioxide loading in

the atmosphere (Govindasamy et al., 2005). As the IAP RAS CM sensitivity to the doubling of the CO_2 concentration in the atmosphere is in the lower half of the range of the current generation of the climate models (1.5–4.5 °C, (Houghton et al., 2001) with an even larger range of sensitivities obtained recently (Stainforth et al., 2005; Forest et al., 2006)), another set of numerical experiments was performed. In this set (denoted as "SENS"), the value of the $\Delta T_{s,g}$ anomaly entering the carbon cycle routine has been arbitrarily multiplied by 1.7 in order to mimic a climate model with a greater sensitivity to the doubling of the CO_2 concentration in the atmosphere ($1.7 \times 2.2\,°C = 3.7\,°C$). This value is not designed to represent any particular climate model, but to yield information about how sensitive the results obtained here are to the basic sensitivity of the climate component of the model. One notes, that the simulations NOCLIM corresponds to the other limiting case of the negligible climate sensitivity of the model to the doubling of the carbon dioxide content in the atmosphere.

In every set of experiments, a subset of parameters $Q_{10,p}$, $Q_{10,r}$, $Q_{10,s}$, k_M and k_D were perturbed. Namely, $Q_{10,p}$ was assigned one of four values (0.8, 1.0, 1.5, and 2.0). $Q_{10,r}$ was also varied between three values, 1.4, 2.15, and 3.0. The corresponding constant for soil respiration $Q_{10,s}$ was assigned one of the four values (1.0, 2.0, 2.4, and 3.0). The half saturation point k_M was pertubed between the values 100, 150, 200, and 450 ppmv. One notes that the constant A_p is also changed in response to the change in k_M in order to retain the pre-industrial level of gross photosynthesis in the model in accordance with the above mentioned values. To test model sensitivity to the choice of constant k_D, as regulating the living biomass with respect to the agricultural activity this constant was also assigned values of 0.0 and 0.27.

All model simulations were initiated from the pre-industrial equilibrated model state. In every simulation, the first model year with non-zero carbon dioxide emissions corresponds to the Julian year 1859. Simulations end in the year corresponding to the Julian year 2100.

The cumulative length of the simulations is 278,784 model years. Such long simulations are currently precluded for state-of-the-art general circulation models due to technical reasons. This advocates the use of climate models of intermediate complexity for the purposes of the present study.

4. The model performance with the standard choice of parameters

Figure 1 presents the simulated atmospheric carbon dioxide concentration for the standard choice of model parameters in comparison with observations collected at the Mauna Loa observatory (Keeling et al., 1996) in 1959–2004. The model reproduces the observed variations of $pCO_{2(a)}$ accurately enough, but underestimates (overestimates) $pCO_{2(a)}$ slightly in the beginning (end) of this period. The absolute error does not exceed 8 ppmv. Errors of this magnitude are typical for the current generation of coupled climate–carbon cycle models (Cox et al., 2000; Brovkin et al., 2002; Dufresne et al., 2002; Friedlingstein et al., 2003; Jones et al., 2003; Matthews et al., 2004, 2005). In the 21st century the model shows the monotonic increase of $pCO_{2(a)}$, in accordance with growing carbon dioxide emissions. The simulated value of $pCO_{2(a)}$, reached in 2100, amounts to 866 ppmv, slightly higher than the value 836 ppmv, attained in the baseline BernCC A2 scenario (Houghton et al., 2001). The value, simulated by IAP RAS CM, is in the range 730–

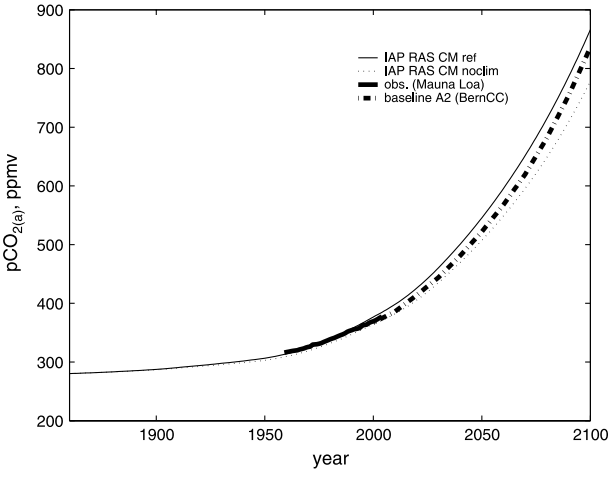

Fig. 1. Simulated atmospheric concentration of carbon dioxide (in ppmv) for the standard model configuration, in the experiments REF (thin solid line) and NOCLIM (thin dotted line), together with the values collected at the Mauna Loa observatory (thick solid line) and BernCC SRES A2 baseline scenario (thick dotted line)

1020 ppmv, identified by C4MIP (Friedlingstein et al., 2006).

Carbon uptake by the ocean in the standard choice of the model parameters amounts to 2.3 and 2.7 GtC/yr in 1980s and 1990s, respectively. This is in the range of the updated observational estimates (1.8 ± 0.8) and (2.1 ± 0.7) GtC/yr, respectively (House et al., 2003). Cumulative oceanic uptake of carbon dioxide for the period 1860–1994 is 107 GtC, which is in agreement with observational estimates of 118 ± 19 GtC (Sabine et al., 2004). For the more recent periods 1980–1999, cumulative oceanic uptake of CO_2 in the model is 49 GtC which deviates only slightly from the range, depicted by Sabine et al. (2004) $(37 \pm 8$ GtC). The simulated terrestrial carbon uptake in the 1980s and 1990s is 1.34 and 1.45 GtC/yr, respectively. The value for the 1980s is within the range 0.3–4.0 GtC/yr figured by House et al. (2003). The value for the 1990s is slightly below the range for the corresponding estimations 1.6–4.8 GtC/yr. However, it falls within the uncertainty range 1.15 ± 0.74 GtC/yr, reported by Patra et al. (2005). The cumulative simulated terrestrial uptakes for 1860–1994 and 1980–1999 (85 and 31 GtC, respectively) fall within the range identified by Sabine et al. (2004) (61–141 and 39 ± 18 GtC, respectively).

In IAP RAS CM, the difference of $pCO_{2(a)}$ between runs REF and NOCLIM is 88 ppmv, again in the range, simulated by the C4MIP models (20–200 ppmv, with the majority of the simulations in the interval 50–100 ppmv (Friedlingstein et al., 2006)). In IAP RAS CM, the gain of this feedback is $g = 0.15$ (the respective C4MIP models' range is 0.04–0.31 with seven of the ten models in the much narrower range 0.1–0.2). As an aside, however, one notes that this rather narrow range stems from different mechanisms of the climate–carbon cycle interaction, related either to terrestrial or oceanic feedbacks. For this reason it suggests much larger intermodel uncertainty than might be inferred at first glance.

The climate–carbon cycle interaction leads to additional global warming of about 0.3 K in 2100 or about 10% of the warming simulated in REF in this year. This additional fractional warming is similar to that simulated by Lenton (2000) but for different emission scenarios.

The difference between the simulations REF and NOCLIM is largely due to the different

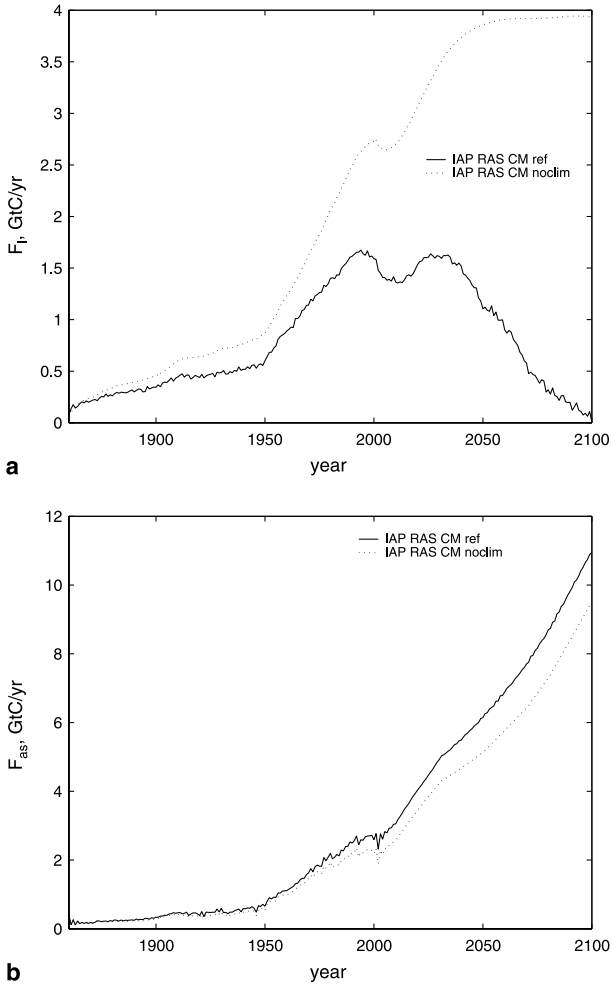

Fig. 2. Simulated CO_2 terrestrial (**a**) and oceanic (**b**) uptakes for the standard model configuration, in the experiments REF (thin solid line) and NOCLIM (thin dotted line)

behaviours of the land carbon uptake, depicted in Fig. 2a. In REF, F_l increases monotonically during the late 19th and the whole 20th centuries reaching maxima in 1994, then decreasing slightly until 2013, and starting to decrease again until 2026. The maxima of F_l in 1994 and 2026 are of comparable magnitudes (1.6–1.7 GtC/yr). The F_l minimum in the early 21st century is due to a mismatch between the historical land use emissions and the SRES A2 scenario, exposed around 2000. Post 2000, terrestrial carbon uptake decreases motonically reaching only 0.1 GtC/yr in 2100. In the simulation NOCLIM, F_l grows monotonically during the whole simulation, apart from the small minimum in 2006. At the end of this simulation, F_l reaches 3.9 GtC/yr. Here, its shape is flat, which is indicative of the saturated

influence of the direct atmospheric CO_2 fertilisation on gross photosynthesis. This is in line with results obtained in C4MIP (Friedlingstein et al., 2006).

To estimate the relevant feedbacks, it is convenient to approximate the terrestrial carbon uptake by the linear relationship

$$F_l = \beta_l \frac{dpCO_{2(a)}}{dt} + \gamma_l \frac{dT_{s,g}}{dt} \quad (7)$$

(Friedlingstein et al., 2003, 2006). The coefficients β_l and γ_l were evaluated, based on the scheme described in Friedlingstein et al. (2003). For the standard model configuration, $\beta_l = 0.52\,\mathrm{GtC/ppmv}$ and $\gamma_l = -82\,\mathrm{GtC/K}$, if one chooses the period 1860–2100 for the approximation. If one selects the period 2000–2100, $\beta_l = 0.64\,\mathrm{GtC/ppmv}$, and $\gamma_l = -100\,\mathrm{GtC/K}$. The values for β_l lie in the lower end of the range depicted by the C4MIP models, 0.2–1.6 GtC/ppmv (Friedlingstein et al., 2006). The values of γ_l are located approximately in the middle part of the respective C4MIP range ($-$(1–177) GtC/K, or, after removing the outlier, $-$(23–177) GtC/K (Friedlingstein et al., 2006)). The coefficient γ_l is more relevant for the climate–carbon cycle feedback, as it directly affects the difference between the simulation with this feedback included or excluded. In contrast, β_l is more relevant to the direct fertilisation effects of $pCO_{2(a)}$.

In contrast, oceanic CO_2 uptake does not show much difference between the two simulations (Fig. 2b). In 2100, they differ no more than 15%, both amounting to about 10 GtC/yr. This value is at the high end of the range, depicted by the C4MIP models (Friedlingstein et al., 2006).

Cumulative terrestrial and oceanic uptake for the standard model configuration in REF amount to 168 and 776 GtC or 8 and 35% of the cumulative emissions, respectively. In the NOCLIM, the corresponding values are 473 GtC (21%) and 661 GtC (30%). These figures are again in the range simulated by the C4MIP models (Friedlingstein et al., 2006).

One concludes that, for the standard configuration of the IAP RAS CM, the intensity of the climate–carbon cycle feedback is controlled by land carbon dynamics. This is again in line with the results of the C4MIP intercomparison, where eight of the ten models attribute this feedback to the terrestrial vegetation-soil dynamics.

As a whole, IAP RAS CM, coupled with the zero-dimensional carbon cycle model, realistically captures the behaviour of the coupled climate–carbon cycle system, forced by the SRES A2 emission scenario. Similar conclusions can be drawn if the model is forced by the combined historical + SRES B2 emission scenario (Mokhov et al., 2006). As a result, IAP RAS CM can be used as a tool for investigating the sensitivity of the climate–carbon cycle feedback to the choice of the governing parameters.

5. The sensitivity of the climate–carbon cycle to the choice of the governing parameters

A preliminary analysis of model output for simulations with different governing parameters has shown that the variations of the two pre-selected parameters, k_M and k_D, only marginally affect the climate–carbon cycle feedback characteristics. Nevertheless, these two parameters do affect the values of β_l. Generally, the latter factor increases with increasing k_M. It also attains higher values for $k_D = 0$, than for $k_D = 0.27$. Additionally, it is sensitive to the amount of carbon dioxide in the atmosphere, representative of the time period when the linearisation is performed. Among the cases studied, the minimum value of β_l is 0.23 GtC/ppmv, and maximum value is 1.61 GtC/ppmv. This includes the whole range exhibited by the C4MIP models, except for the single model corresponding to $\beta_l = 2.8\,\mathrm{GtC/ppmv}$ (Friedlingstein et al., 2006).

The relative insensitivity of the climate–carbon cycle feedback strength to the choice of k_M and k_D with a rather wide range of the respective variations of β_l again confirms that β_l is more relevant to the fertilisation effect of CO_2 and to the general increase of the atmospheric CO_2 concentration during the course of the model run, than to the climate–carbon cycle feedback strength. The reason for this behaviour in IAP RAS CM is greater litterfal and greater soil respiration under enhanced fertilisation. In turn, changes in litterfal and soil respiration are due to a recalibration of A under perturbed k_M.

In contrast, all Q_{10} drastically affect the results of the climate–carbon cycle feedback characteristics. As expected, the difference $\Delta pCO_{2(a)}^{xxx}$, $xxx = REF, SENS$ between either REF or SENS on one hand, and NOCLIM on the other, in-

creases (decreases) with increasing $Q_{10,s}$ ($Q_{10,p}$). It also increases with increasing $Q_{10,r}$. Climate sensitivity increases the magnitude of the difference between the climate change and the NOCLIM simulations, enhancing magnitudes of $\Delta pCO_{2(a)}^{SENS}$ with respect to $\Delta pCO_{2(a)}^{REF}$ with the same governing parameters of the carbon cycle. The latter enhancement is almost linear, as the ratio $\Delta pCO_{2(a)}^{SENS}/\Delta pCO_{2(a)}^{REF}$ scatter only slightly around the value 1.7.

The values of $\Delta pCO_{2(a)}^{xxx}$ span a rather broad interval, from -118 up to 445 ppmv. Nevertheless, one may not consider the whole interval, because the simulations have to fulfil the important constraint of the realism for the 20th century simulation. In the present paper, this constraint is formulated via two terms. Firstly, the maximum deviation of the simulated $pCO_{2(a)}$ from the Mauna Loa observations are not allowed to exceed some prescribed value $\varepsilon_{pCO_{2(a)}}$. It is impossible to zero this value due to the finiteness of the grid in the parameter space. The minimum studied here, $\varepsilon_{pCO_{2(a)}} = 2$ ppmv, roughly corresponds to the observed year-to-year variations of $pCO_{2(a)}$ (Zeng et al., 2005). Secondly, simulated terrestrial and oceanic carbon uptake in the 1980s and 1990s must be in the range figured in House et al. (2003) (see above). These two terms may be considered either separately or in combination. The results are presented in Table 1. From this Table, one can see that this constraint can narrow the uncertainty range for the climate–carbon cycle feedback considerably. In particular, if one imposes only the $\varepsilon_{pCO_{2(a)}}$-term with the allowed range of $pCO_{2(a)}$ is -45 to $+450$ ppmv. Alternatively, if one imposes the uptake term, the range is -118 to $+385$ ppmv. In this, the terrestrial uptake leads to a stronger constraint than the oceanic. This is additionally illustrated in Fig. 3 for the particular case when only $Q_{10,p}$ and $Q_{10,s}$

Table 1. Ranges of the climate–carbon cycle feedback strength in terms of $\Delta pCO_{2(a)}$, for different values of the allowed deviations $\varepsilon_p CO_{2(a)}$ of the simulated concentration of the carbon dioxide in the atmosphere from the Mauna Loa observations for 1959–2000, and for different constraints on the simulated uptakes

$\varepsilon_p CO_{2(a)}$ (ppmv)	None	F_l	F_{as}	F_l and F_{as}
None	-118 to $+445$	-118 to $+385$	-118 to $+403$	-118 to $+385$
10	-98 to $+403$	-98 to $+385$	-98 to $+403$	-98 to $+385$
5	-65 to $+403$	-65 to $+385$	-65 to $+403$	-65 to $+385$
2	-45 to $+403$	-45 to $+280$	-45 to $+403$	-45 to $+280$

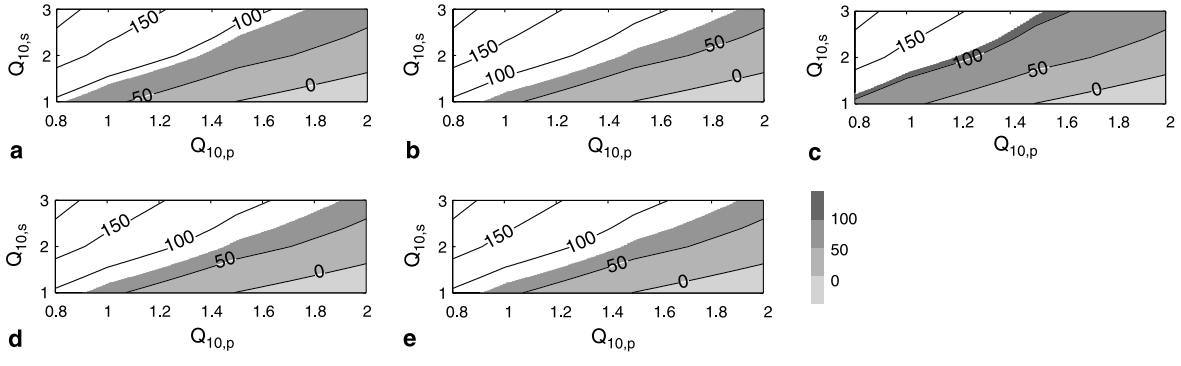

Fig. 3. Difference between the simulated atmospheric CO_2 concentration (ppmv) between experiments REF and NOCLIM in 2100 as a function of Q_{10}-factors for photosynthesis (abscissae) and soil respiration (ordinates) keeping all other model parameters at the standard values. Simulations fulfilling the specified below conditions are shaded in gray. At individual plots the condition to be fulfilled is (**a**) the simulated $pCO_{2(a)}$ must not deviate from the Mauna Loa observations more than on 10 ppmv; (**b**) the simulated terrestrial uptakes F_l in 1980s and 1990s must be in the range reported in House et al. (2003); (**c**) the simulated oceanic uptakes F_{as} in 1980s and 1990s must be in the range reported in House et al. (2003); (**d**) both F_l and F_{as} in 1980s and 1990s must be in the range reported in House et al. (2003); (**e**) the simulated $pCO_{2(a)}$ must not deviate from the Mauna Loa observations more than on 10 ppmv and both the F_l and F_{as} in 1980s and 1990s must be in the range reported in House et al. (2003)

are varied while other model parameters are retained at their standard values. It is notable that even the relatively strong version of this constraint, corresponding to the maximum allowed deviations from the Mauna Loa observations $\varepsilon_{pCO_{2(a)}} = 2$ppmv, cannot exclude the possibility of the negative feedback (with the magnitude up to 45 ppmv). It is also unable to exclude the highest positive feedback value among those simulated by the C4MIP models. This is true even for the simulation sets REF-NOCLIM, while, generally, the intensity of the climate–carbon cycle feedback (either positive or negative) is higher for the pairs SENS-NOCLIM.

The simulated range for the feedback gain is -0.30 to $+0.55$ if no constraint is imposed. In turn, if $\varepsilon_{pCO_{2(a)}} = 2$ ppmv and both terrestrial and oceanic uptakes are constrained, the corresponding range is -0.11 to $+0.41$.

Intensity of the climate–carbon cycle feedback, expressed either in terms of $\Delta pCO_{2(a)}$, or in terms of the corresponding gains, depends almost linearly on the values of γ_l. Figure 4 shows such dependence for the pairs of the simulations REF and NOCLIM, corresponding to the same choice of the governing parameters. The scatter, exhibited by the points in this Fig., is due to different choices of k_D and k_M. The respective dependence for the pairs SENS-NOCLIM is almost indistinguishable from that presented in this Fig., and is not shown. This dependence again confirms that the climate–carbon cycle feedback is mainly associated with γ_l rather than with β_l. Additionally, the corresponding values simulated by the C4MIP model ensemble (Friedlingstein et al., 2006) are depicted in Fig. 4 as blue circles. The latter symbols generally follow those simulated by IAP RAS CM. This again confirms that the global output from the C4MIP ensemble can be approximated by a simple zero-dimensional carbon cycle model, coupled with the climate model of intermediate complexity.

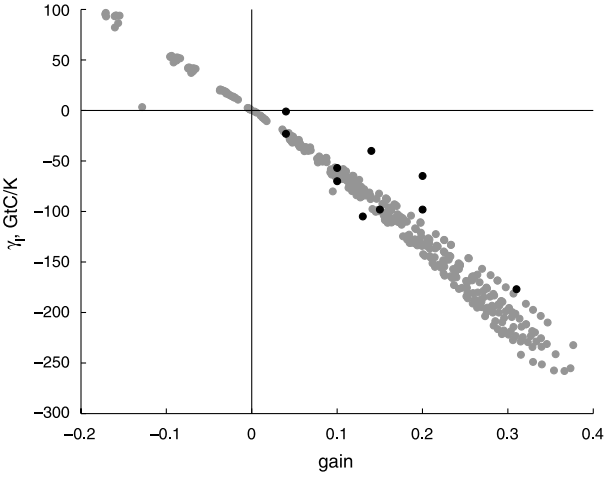

Fig. 4. Dependence of the coefficient γ_l on the climate–carbon cycle feedback gains, evaluated for the corresponding pair of the experiments REF and NOCLIM (gray circles) together with the corresponding values, simulated by the C4MIP models (black circles)

Table 2 shows the allowed ranges for the coefficients γ_l, evaluated for 2000–2100, which are dependent on the allowed maximum deviations of the simulated $pCO_{2(a)}$ from the Mauna Loa observations. As it was for $\Delta pCO_{2(a)}$, this constraint allows a considerable narrowing of the possible range of γ_l. If no constraint is imposed, the simulated range is -415 to $+167$ GtC/K. For the strongest studied constraint, $\varepsilon_p CO_{2(a)} = 2$ ppmv, with the unconstrained uptakes, the largest (in magnitude) negative values of γ_l do not change drastically, but the largest positive values are reduced to 62 GtC/K. If the simulated $pCO_{2(a)}$ is unconstrained and while both terrestrial and oceanic uptakes are constrained, the maximum positive values are unchanged while the strongest negative values become slightly weaker, -387 GtC/K. Again, the terrestrial uptake serves as a stronger constraint in comparison

Table 2. Ranges of the coefficients γ_l (see (7)) for different values of the allowed deviations $\varepsilon_p CO_{2(a)}$ of the simulated concentration of the carbon dioxide in the atmosphere from the Mauna Loa observations for 1959–2000, and for different constraints on the simulated uptakes

$\varepsilon_p CO_{2(a)}$ (ppmv)	None	F_l	F_{as}	F_l and F_{as}
None	−415 to +167	−387 to +167	−401 to +167	−387 to +167
10	−401 to +134	−387 to +134	−401 to +134	−387 to +134
5	−401 to +89	−387 to +134	−401 to +134	−387 to +134
2	−401 to +62	−288 to +62	−401 to +62	−288 to +62

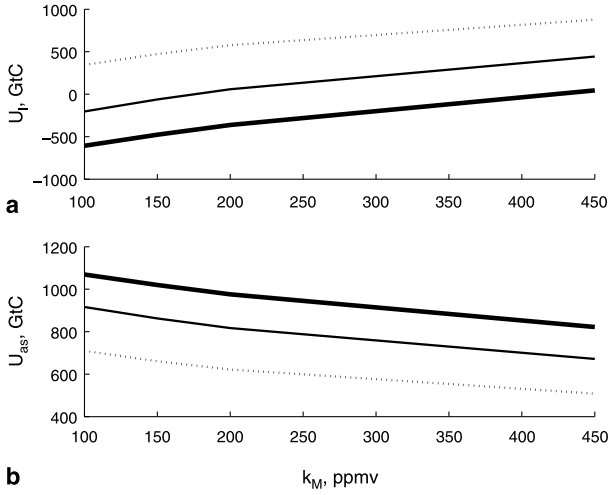

Fig. 5. Dependence of the cumulative terrestrial (**a**) and oceanic (**b**) CO_2 uptakes on the half-saturation point of fertilisation k_M, keeping the standard values for the other model parameters, in experiments REF (thin solid line), SENS (thick solid line), and NOCLIM (dotted line)

to the oceanic one. If $\varepsilon_p CO_{2(a)} = 2\,\text{ppmv}$ and both F_l and F_{as} are constrained, the respective range is -288 to $+62\,\text{GtC/K}$. As found previously, the simulated range is broader than the respective C4MIP range (see above).

Figure 5a shows the dependence of the cumulative (summed over 1860–2100) terrestrial uptake U_l on the land biota fertilisation half-saturation point k_M, keeping other model parameters at their standard values. Generally, larger k_M tends to make cumulative terrestrial uptake more positive, increasing the positive uptake and diminishing the negative uptake. While precise values depend on model sensitivity, it is notable that three curves in Fig. 5a are almost parallel to each other, indicating that partial derivative of the cumulative terrestrial uptake on the half-saturation point is almost independent of other model parameters. For $k_D = 0$ (not shown) cumulative terrestrial uptake is larger than for $k_D = 0.27$. In principle, increase of the half-saturation point directly diminishes plant photosynthesis. However, in the present paper, this influence is compensated by the corresponding change of A_p to ensure the equilibrated pre-industrial model state remains unchanged. In the following course of particular REF simulation, smaller k_M leads to the faster build up of carbon dioxide in the atmosphere, stronger warming and enhanced photosynthesis.

Variations in the model parameters governing the land biota half-saturation point and the vegetation losses due to land use, lead to corresponding variations in $pCO_{2(a)}$. This, in turn, leads to the variations of the cumulative oceanic uptakes U_{as} (Fig. 5b). Larger terrestrial uptake leads to the smaller airborne fraction of the anthropogenically emitted carbon dioxide. The smaller growth of $pCO_{2(a)}$ outweighs the direct influence of temperature on F_{as} and leads, in turn, to smaller oceanic uptake. As for the terrestrial cumulative uptake, cumulative oceanic uptake varies across a rather broad interval and depends strongly on the climate model sensitivity. Nevertheless, its partial derivative on the half-saturation point is almost independent of other model parameters. For $k_D = 0$ (not shown) cumulative oceanic uptake is smaller than for $k_D = 0.27$. This is again

Table 3. Ranges of the cumulative terrestrial and oceanic uptakes of CO_2 (in GtC) for 1860–2100 and the corresponding atmospheric CO_2 storage for different values of the allowed deviations $\varepsilon_p CO_{2(a)}$ of the simulated concentration of the carbon dioxide in the atmosphere from the Mauna Loa observations for 1959–2000, and for different constraints on the simulated uptakes. The corresponding ranges for the landborne, oceanborne and airborne fractions (per cents) of the emitted CO_2 are figured in parentheses

$\varepsilon_p CO_{2(a)}$ (ppmv)	Terrestrial storage		Oceanic storage		Atmospheric storage	
	None	F_l and F_{as}	None	F_l and F_{as}	None	F_l and F_{as}
None	−944 to +1344	−232 to +1167	+332 to +1198	+398 to +926	+272 to +1970	+657 to +1529
	(−42 to +60)	(−10 to +53)	(+15 to +54)	(+18 to +42)	(+12 to +89)	(+30 to +69)
10	−392 to +684	−232 to +684	+581 to +987	+581 to +926	+905 to +1628	+958 to +1529
	(−18 to +31)	(−10 to +31)	(+26 to +44)	(+26 to +42)	(+41 to +73)	(+43 to +69)
5	−298 to +569	−232 to +569	+624 to +951	+624 to +926	+1030 to +1570	+1030 to +1529
	(−13 to +26)	(−10 to +26)	(+28 to +43)	(+28 to +42)	(+46 to +71)	(+46 to +69)
2	−295 to +500	−142 to +500	+650 to +950	+650 to +892	+1073 to +1568	+1073 to +1473
	(−13 to +22)	(−6 to +22)	(+29 to +43)	(+29 to +40)	(+48 to +71)	(+48 to +66)

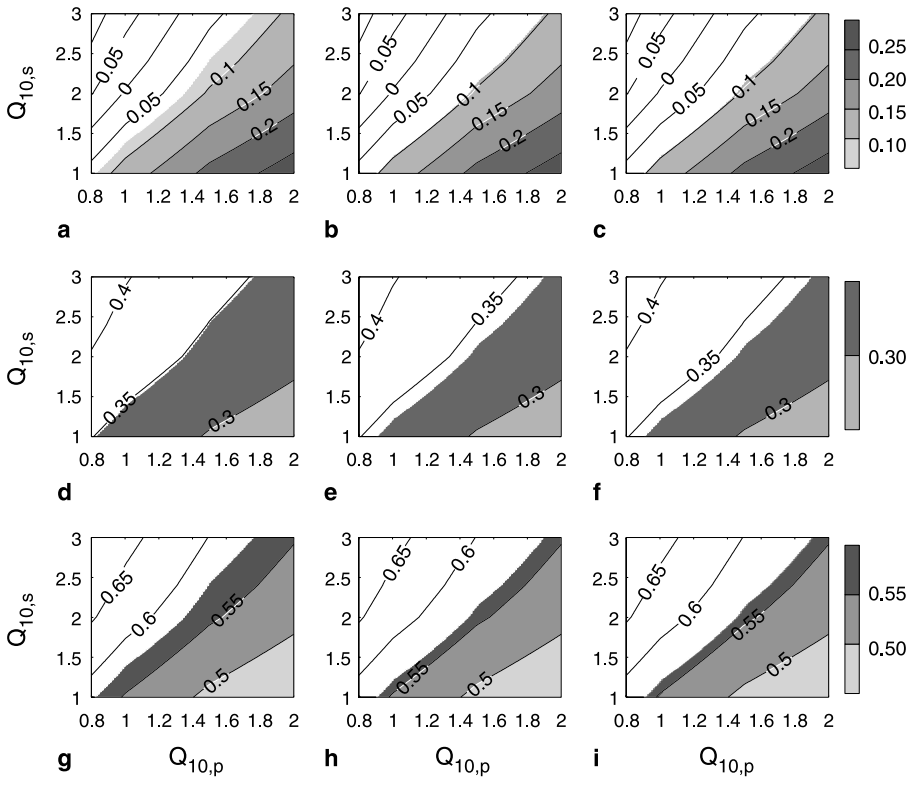

Fig. 6. Dependence of the landborne (**a**–**c**), oceanborne (**d**–**f**), and airborne (**g**–**i**) fractions of the emitted in 1860–2100 CO_2 on the Q_{10}-factors for photosynthesis (abscissae) and soil respiration (ordinates) at experiments REF keeping all other model parameters at the standard values. The simulations fulfilling the specified below conditions are shaded in gray. At individual plots the condition to be (**a**, **d**, **g**) the simulated $p\mathrm{CO}_{2(a)}$ must not deviate from the Mauna Loa observations more than on 10 ppmv; (**b**, **e**, **h**) the simulated terrestrial (F_l) and oceanic (F_{as}) uptakes in 1980s and 1990s must be in the range reported in House et al. (2003); (**c**, **f**, **i**) the simulated $p\mathrm{CO}_{2(a)}$ must not deviate from the Mauna Loa observations more than on 10 ppmv and both F_l and F_{as} in 1980s and 1990s must be in the range reported in House et al. (2003)

the direct result of the enhanced (by the larger values of k_D) terrestrial uptakes, leading to the smaller $p\mathrm{CO}_{2(a)}$.

In Table 3 (and in Fig. 6 for the particular case when only $Q_{10,p}$ and $Q_{10,s}$ are varied while other model parameters are kept at their standard values) the landborne, oceanborne and airborne fractions of anthropogenically emitted carbon dioxide (including that due to land use) for 1860–2100 are shown. If no constraint is imposed, the landborne fraction varies in a rather broad range -42 to $+60\%$ which is much wider than that simulated by the C4MIP models, 1–45% (Friedlingstein et al., 2006). If one constrains the simulated uptake, the respective range becomes narrower, -10 to $+53\%$, but is still wider than found in C4MIP. However, if one constrains the simulated $p\mathrm{CO}_{2(a)}$ with $\varepsilon_p\mathrm{CO}_{2(a)} = 2$ ppmv, the allowed range becomes -13 to $+22\%$ and is narrower than that simulated by the C4MIP ensemble. For the strong constraint $\varepsilon_p\mathrm{CO}_{2(a)} = 2-10$ ppmv, this range is even narrower, and some of the C4MIP simulations lie outside it. If both $p\mathrm{CO}_{2(a)}$ and uptakes are constrained, the range for the landborne fraction is -6 to $+22\%$.

The oceanborne fraction of the emitted carbon dioxide (Fig. 6 and Table 3), if unconstrained, also varies over a rather wide range, 15–54%, which is wider than the corresponding C4MIP range 15–35% (Friedlingstein et al., 2006). However, if one constrains the uptakes, the range shrinks to 18–42% with one C4MIP model lying outside this range. If one imposes the $\varepsilon_p\mathrm{CO}_{2(a)}$-constraint, the respective range becomes narrower (for instance, 29–43% for $\varepsilon_p\mathrm{CO}_{2(a)} = 2$ ppmv). The most narrow range is obtained if both the simulated $p\mathrm{CO}_{2(a)}$ and uptakes are constrained: 29–40% for $\varepsilon_p\mathrm{CO}_{2(a)} = 2$ ppmv.

The airborne fraction of the emitted carbon dioxide (Fig. 6 and Table 3), if unconstrained,

is 12–89% which is wider than the corresponding C4MIP range, 42–72% (Friedlingstein et al., 2006). If the uptakes are constrained, the simulated range in the present paper becomes 30–69%. By decreasing $\varepsilon_p CO_{2(a)}$ with the unconstrained uptakes, the range may be narrowed to 48–71%. With both terms constrained, this range is 48–66%.

In (Lenton, 2000), a feedback analysis was performed by perturbing one of the temperature dependences of photosynthesis, biota and soil respiration. Additionally, parameter k_M was perturbed in order to match the observed value of $pCO_{2(a)}$ in 1990. The goal of analysis, in particular, was to study the response of the maximum value of terrestrial carbon uptake to such perturbations. In the present paper, similar analysis has been performed to that conducted by Lenton (2000) where characteristics were achieved only in extended scenarios with zeroed emissions in the 22th–23rd centuries and cannot be compared directly. One has to be cautioned that the emission scenarios in the 21st century are quite different: Lenton (2000) utilised the IS92a scenario (Houghton et al., 1992) with carbon dioxide emissions systematically smaller than those characteristic of the SRES A2 scenario. In the subsequent paragraph, the results are presented for $\varepsilon_p CO_{2(a)} = 5$ ppmv.

In this comparison, for the smallest studied $Q_{10,p} = 0.8$, the maximum value of F_l, $F_{l,m}$ is $1.3-3.3\,\mathrm{GtC/yr}$ depending on k_M, k_D, and effective climate sensitivity if the uptakes are unconstrained and $1.7-3.3\,\mathrm{GtC/yr}$ if both terrestrial and oceanic uptakes are constrained. Lenton (2000) reported values of $2.14\,\mathrm{GtC/yr}$ but for $Q_{10,p} = 1.0$ (in the present paper the respective ranges of maximum achieved for this value of $Q_{10,p}$ are just marginally different from those for $Q_{10,p} = 0.8$). For the largest studied $Q_{10,p} = 2.0$, the range of $F_{l,m}$ is $1.8-3.9\,\mathrm{GtC/yr}$, irrespective of the imposed constraint on the uptakes; the corresponding value reported in Lenton (2000) is $2.91\,\mathrm{GtC/yr}$. For the smallest studied $Q_{10,r} = 1.4$, the range of $F_{l,m}$ is $1.7-4.1\,\mathrm{GtC/yr}$ ($1.8-5.0\,\mathrm{GtC/yr}$) again irrespective of the imposed constraint on the uptakes. For the largest studied $Q_{10,r} = 3.0$ the corresponding range is $1.5-3.7\,\mathrm{GtC/yr}$ ($1.7-3.7\,\mathrm{GtC/yr}$) if the uptakes are unconstrained (constrained). Lenton (2000) published values of 2.74 and $2.22\,\mathrm{GtC/yr}$ for lower and upper limits of the biota respiration temperature response, respectively. Similarly, for $Q_{10,s} = 1.0$ the range of $F_{l,m}$ is $2.6-4.0\,\mathrm{GtC/yr}$ ($1.8-5.0\,\mathrm{GtC/yr}$) irrespective of the imposed constraint on the uptakes, and for $Q_{10,s} = 3.0$, the range is $1.5-3.9\,\mathrm{GtC/yr}$ ($1.7-3.9\,\mathrm{GtC/yr}$) if the uptakes are unconstrained (constrained). The corresponding Lenton (2000) values are 2.81 and $2.16\,\mathrm{GtC/yr}$. It is notable that the scatter of $F_{l,m}$ due to variations of k_D, k_M, and effective climate sensitivity is large enough to make the ranges corresponding to the lower and upper limits of particular Q_{10} not so easily distinguishable between each other even in the case where both the simulated $pCO_{2(a)}$ and uptakes are constrained.

6. Discussion and conclusions

In this paper, simulations have been performed with a coupled climate–carbon cycle model. The climatic component consists of the climate model of intermediate complexity IAP RAS CM and the carbon cycle component is formulated as a zero-dimensional model. Its terrestrial module is subjected to a Michaelis-Menten type fertilisation law and Q_{10}-relationships for the temperature dependence of plant photosynthesis, living biota respiration, and soil respiration. The oceanic carbon cycle module is formulated in a bilinear fashion. The model is forced by historical changes in industrial and land use emissions for the second half of the 19th and the entire 20th centuries, and by the emission scenario SRES A2 for the 21st century. Numerous simulations have been performed, perturbing the governing parameters of the terrestrial carbon cycle. In addition to this, the climate part is perturbed, by either zeroing or artificially increasing the climate model sensitivity to the varying atmospheric concentration of carbon dioxide.

For the standard set of governing parameters, the model realistically captures the main features of the Earth's observed carbon cycle, such as the observed $pCO_{2(a)}$ changes during the second half of the 20th century and the estimated terrestrial and oceanic uptakes of carbon dioxide.

By performing the above mentioned model perturbations, it has been possible to mimic most of the range of the climate–carbon cycle feedback characteristics found in the C4MIP simulations within a single model. In particular,

globally averaged output of the different C4MIP models can be approximated by different values of the governing parameters of a climate–carbon cycle system.

Perturbing the above mentioned governing parameters, one obtains a wide range of climate–carbon cycle feedback strengths. Even the sign of this feedback can vary, changing from positive to negative, independent of the particular set of the governing parameters.

If the performed simulations are subjected to the constraint of the maximum allowed deviation of the simulated $p\mathrm{CO}_{2(a)}$ from the observed values (measured at the Mauna Loa observatory during the second half of the 20th century), and/or to the constraint that simulated terrestrial and oceanic uptakes in the 1980s and 1990s must be in the range published in House et al. (2003), it is possible to rule out some of the simulations performed in the present paper, and narrow the corresponding uncertainty range. Among these constraints, the simulated $p\mathrm{CO}_2(a)$ and uptakes are both important. However, the terrestrial uptakes constrain the simulations more effectively than the oceanic ones.

Both these constraints were not imposed in the published analysis of the C4MIP simulations. Some of the C4MIP simulations appear to be outside the range of the constrained simulations presented here. Nevertheless, the authors are not dismissing any of the C4MIP simulations, taking into account the extreme simplicity of the carbon cycle scheme, used in the present paper. In particular, the linear formulation of the oceanic carbon cycle may break down for the climates which are substantially warmer than the present-day, leading to saturation effects in the oceanic carbon storage. The terrestrial carbon cycle used here may also behave unrealistically in a climate which is markedly warmer than the present-day, owing to the above mentioned low value of the fertilisation half-saturation constant.

The role of the uncertainty of the behaviour of the ocean carbon uptake is beyond the scope of this study. Basically, this choice is dictated by the extreme simplicity of the ocean carbon uptake formulation used in the present paper. However, some notes can be added on the possible influence of the ocean on the carbon cycle. Cumulative oceanic uptake can be diagnosed in a way similar to (7), but with β_l, γ_l, and $T_{s,g}$ replaced by β_{oc}, γ_{oc}, and $T_{oc,g}$, respectively. From (6) one finds $u_c = \gamma_{oc}$, $u_T = \beta_{oc}$. As a result, perturbations of u_c and u_T would result in the ranges which are similar to those figured in Table 2, but with γ_l replaced by $\gamma_l + \gamma_{oc}$.

In the present paper, the imposed constraints on the simulated atmospheric carbon dioxide content, and terrestrial and oceanic uptakes, while appearing to be useful, are still unable to rule out both extremely strong positive and modest negative positive climate–carbon cycle feedback. This is not surprising, considering the relative smallness of the climate and carbon cycle perturbations in the currently available observations relative to those expected in the 21st century. Moreover, in addition to the above mentioned sources of simulation uncertainty, uncertainty of the emissions or unresolved climate forcings and processes are not considered in the paper.

The conclusion that the constraint imposed by the currently available carbon cycle observational estimates on the future is weak is also shared by Jones et al. (2006). They showed that ''the observational record proves to be insufficient to tightly constrain carbon cycle processes or future feedback strength with implications for climate–carbon cycle model evaluation''. Melnikov and O'Neill (2006) were able to accurately reproduce the 20th century course of the carbon cycle characteristics with a model accounting for only direct CO_2 influence on F_l and F_{as} without considering respective climate feedbacks. It is notable, that zero intensity of the climate–carbon cycle lies within the estimated range in the present paper. For this reason, the results by Melnikov and O'Neill (2006) are in accord with the results of the present paper.

Acknowledgements

The authors are indebted to V. Brovkin, P. Friedlingstein, L. Golubyatnikov, S. V. Venevsky, and E. M. Volodin for useful discussions on the topic of the manuscript. The constructive comments of the anonymous referees were very helpful in improving the paper. This work has been supported by the Programs of the Russian Ministry for Science and Education, Russian Federal Agency for Science and Innovations and the Russian Academy of Sciences, by the President of Russia grant 4166.2006.5, and by the Russian Foundation for Basic Research (grants 05-05-64907, 05-05-65167, and 05-05-08045).

References

Adams B, White A, Lenton TM (2004) An analysis of some diverse approaches to modelling terrestrial net primary productivity. Ecol Mod 177: 353–391

Brovkin V, Bendtsen J, Claussen M, Ganopolski A, Kubatzki C, Petoukhov V, Andreev A (2002) Carbon cycle, vegetation, and climate dynamics in the Holocene: experiments with the CLIMBER-2 model. Glob Biogeochem Cycles 16: 1139

Brovkin V, Sitch S, Bloh von W, Claussen M, Bauer E, Cramer W (2004) Role of land cover changes for atmospheric CO_2 increase and climate change during the last 150 years. Glob Change Biol 10: 1253–1266

Budyko MI, Izrael YA (eds) (1991) Anthropogenic climate change. Tucson: Arizona Univ. Press

Cox PM, Betts RA, Collins M, Harris PP, Huntingford C, Jones CD (2004) Amazonian forest dieback under climate–carbon cycle projections for the 21st century. Theor Appl Climatol 78: 137–156

Cox PM, Betts RA, Jones CD, Spall SA, Totterdell IJ (2000) Acceleration of global warming due to carbon-cycle feedbacks in a coupled climate model. Nature 408: 184–187

Dufresne J-L, Friedlingstein P, Berthelot M, Bopp L, Ciais P, Fairhead L, Le Treut H, Monfray P (2002) On the magnitude of positive feedback between future climate change and the carbon cycle. Geophys Res Lett 29: 1405

Eliseev AV, Mokhov II, Karpenko AA (2006) Variations of climate and carbon cycle in the 20th–21st centuries in climate model of intermediate complexity. Izvestiya, Atmos Ocean Phys 42 (in press)

Farquhar GD, Caemmerer von S, Berry JA (1980) A biochemical model of photosynthetic CO_2 assimilation in leaves of c_3 species. Planta 149: 78–90

Forest CE, Stone PH, Sokolov AP (2006) Estimated PDFs of climate system properties including natural and anthropogenic forcings. Geophys Res Lett 33: L01705

Friedlingstein P, Bopp L, Ciais P, Dufresne J-L, Fairhead L, Le Treut H, Monfray P, Orr J (2001) Positive feedback between future climate change and the carbon cycle. Geophys Res Lett 28: 1543–1546

Friedlingstein P, Cox P, Betts R, Bopp L, Bloh von W, Brovkin V, Doney S, Eby M, Fung I, Govindasamy B, John J, Jones C, Joos F, Kato T, Kawamiya M, Knorr W, Lindsay K, Matthews HD, Raddatz T, Rayner P, Reick C, Roeckner E, Schnitzler K-G, Schnur R, Strassmann K, Weaver AJ, Yoshikawa C, Zeng N (2006) J Climate Climate–carbon cycle feedback analysis, results from the C4MIP model intercomparison (accepted)

Friedlingstein P, Dufresne J-L, Cox PM, Rayner P (2003) How positive is the feedback between climate change and the carbon cycle? Tellus 55B: 692–700

Govindasamy B, Thompson S, Mirin A, Wickett M, Caldeira K, Delire C (2005) Increase of carbon cycle feedback with climate sensitivity: results from a coupled climate and carbon cycle model. Tellus 57B: 153–163

Handorf D, Petoukhov VK, Dethloff K, Eliseev AV, Weisheimer A, Mokhov II (1999) Decadal climate variability in a coupled atmosphere-ocean climate model of moderate complexity. J Geophys Res 104: 27253–27275

Houghton JT, Callander BA, Varney SK (eds) (1992) Climate change: the supplementary report to the IPCC scientific assessment, intergovernmental panel on climate change. Cambridge: Cambridge University Press, pp 198

Houghton JT, Ding Y, Griggs DJ, Noguer M, Linden van der PJ, Dai X, Maskell K, Johnson CA (eds) (2001) Climate change 2001: the scientific basis contribution of Working Group I to the Third Assessment Report of the Intergovernmental Panel on Climate Change. Cambridge, New York: Cambridge University Press, 881 pp

Houghton RA (2003) Revised estimates of the annual net flux of carbon to the atmosphere from changes in land use and land management 1850–2000. Tellus 55B: 378–390

House JI, Prentice IC, Ramankutty N, Houghton RA, Heimann M (2003) Reconciling apparent inconsistencies in estimates of terrestrial CO_2 sources and sinks. Tellus 55B: 345–363

Huntingford C, Cox PM, Lenton TM (2000) Contrasting responses of a simple terrestrial ecosystem model to global change. Ecol Mod 177: 41–58

Huntingford C, Harris PP, Gedney N, Cox PM, Betts RA, Marengo JA, Gash JHC (2004) Using a GCM analogue model to investigate the potential for Amazonian forest dieback. Theor Appl Climatol 78: 177–185

Jones CD, Cox PM (2001) Constraints on the temperature sensitivity of global soil respiration from the observed interannual variability in atmospheric CO_2. Atmos Sci Lett

Jones CD, Cox PM, Essery RLH, Roberts DL, Woodage MJ (2003) Strong carbon cycle feedbacks in a climate model with interactive CO_2 and sulphate aerosols. Geophys Res Lett 30: 1479

Jones CD, Cox PM, Huntingford C (2006) Climate–carbon cycle feedbacks under stabilisation: uncertainty and observational constraints. Tellus 58B (in press)

Jones PD, New M, Parker DE, Martin S, Rigor IG (1999) Surface air temperature and its changes over the past 150 years. Rev Geophys 37: 173–199

Keeling CD, Chine JFS, Whorf TP (1996) Increased activity of northern vegetation inferred from atmospheric CO_2 measurements. Nature 382: 146–149

Kwon O, Schnoor JL (1994) Simple global carbon model: The atmosphere-terrestrial biosphere-ocean interaction. Glob Biogeochem Cycles 8: 295–305

Le Quéré C, Aumant O, Bopp L, Bousquet P, Ciais P, Francey R, Heimann M, Keeling RF, Kheshgi H, Peylin P, Piper SC, Prentice IC, Rayner P (2003) Two decades of ocean CO_2 sink and variability. Tellus 55B: 649–656

Lenton TM (2000) Land and ocean carbon cycle feedback effects on global warming in a simple Earth system model. Tellus 52B: 1159–1188

Lloyd J, Taylor JA (1994) On the temperature dependence of soil respiration. Func Ecol 8: 315–323

Marland G, Boden TA, Andres RJ (2005) Global, regional, and national CO_2 emissions. Trends: a compendium of data on global change. carbon dioxide information analysis center. Oak Ridge National Laboratory, U.S. Department of Energy, Oak Ridge, Tenn

Matthews HD, Weaver AJ, Meissner KJ (2005) Terrestrial carbon cycle dynamics under recent and future climate change. J Climate 18: 1609–1628

Matthews HD, Weaver AJ, Meissner KJ, Gillett NP, Eby M (2004) Natural and anthropogenic climate change: incorporating historical land cover change, vegetation dynamics and the global carbon cycle. Clim Dyn 22: 461–479

Melillo JM, Steudler PA, Aber JD, Newkirk K, Lux H, Bowles FP, Catricala C, Magill A, Ahrens T, Morrisseau S (2002) Soil warming and carbon-cycle feedbacks to the climate system. Science 298: 2173–2176

Melnikov NB, O'Neill BC (2006) Learning about the carbon cycle from global budget data. Geophys Res Lett 33: L02705

Mokhov II, Demchenko PF, Eliseev AV, Khon VCh, Khvorostyanov DV (2002) Estimation of global and regional climate changes during the 19th–21st centuries on the basis of the IAP RAS model with consideration for anthropogenic forcing. Izvestiya, Atmos Ocean Phys 38: 555–568

Mokhov II, Eliseev AV, Demchenko PF, Khon VCh, Akperov MG, Arzhanov MM, Karpenko AA, Tikhonov VA, Chernokulsky AV, Sigaeva EV (2005) Climate changes and their assessment based on the IAP RAS global model simulations. Doklady Earth Sci 402: 591–595

Mokhov II, Eliseev AV, Karpenko AA (2006) Sensitivity of the IFA RAN Global Climate Model with an interactive carbon cycle to anthropogenic influence. Doklady Earth Sci 407: 424–428

Patra PK, Maksyutov S, Ishizawa M, Nakazawa T, Takahashi T, Ukita J (2005) Interannual and decadal changes in the sea–air CO_2 flux from atmospheric CO_2 inverse modeling. Glob Biogeochem Cycles 19: GB4013

Petoukhov V, Claussen M, Berger A, Crucifix M, Eby M, Eliseev AV, Fichefet T, Ganopolski A, Goosse H, Kamenkovich I, Mokhov II, Montoya M, Mysak LA, Sokolov A, Stone P, Wang Z, Weaver A (2005) EMIC intercomparison project (EMIP-CO_2): Comparative analysis of EMIC simulations of current climate and equilibrium and transient reponses to atmospheric CO_2 doubling. Clim Dyn 25: 363–385

Petoukhov VK, Mokhov II, Eliseev AV, Semenov VA (1998) The IAP RAS global climate model. Dialogue-MSU, Moscow, pp 110

Plattner G-K, Joos F, Stocker TF (2002) Revision of the global carbon budget due to changing air–sea oxygen fluxes. Glob Biogeochem Cycles 16: 1096

Raich JW, Schlesinger WH (1992) The global carbon dioxide flux in soil respiration and its relationship to vegetation and climate. Tellus 44B: 81–99

Sabine CL, Feely RA, Gruber N, Key RM, Lee K, Bullister JL, Wanninkhof R, Wong CS, Wallace DWR, Tilbrook B, Millero FJ, Peng T-H, Kozyr A, Ono T, Rios AF (2004) The oceanic sink for anthropogenic CO_2. Science 305: 367–371

Siegenthaler U, Sarmiento JL (1993) Atmospheric carbon dioxide and the ocean. Nature 365: 119–125

Stainforth DA, Aina T, Christensen C, Collins M, Faull N, Frame DJ, Kettleborough JA, Knight S, Martin A, Murphy JM, Piani C, Sexton D, Smith LA, Spicer RA, Thorpe AJ, Allen MR (2005) Uncertainty in predictions of the climate response to rising levels of greenhouse gases. Nature 433: 403–406

Svirezhev YU, Krapivin VF, Tarko AM (1985) Modeling of the main biosphere cycles. In: Malone TF, Roederer JS (eds) Global change. Cambridge: Cambridge University Press, pp 298–313

Thomas H, England MH, Ittekkot V (2001) An off-line 3D model of anthropogenic CO_2 uptake by the oceans. Geophys Res Lett 28: 547–550

Trumbore SE, Chadwick OA, Amundsen R (1996) Rapid exchange between soil carbon and atmospheric carbon dioxide driven by temperature change. Science 272: 393–396

Zeng N, Qian H, Roedenbeck C, Heimann M (2005) Impact of 1998–2002 midlatitude drought and warming on terrestrial ecosystem and the global carbon cycle. Geophys Res Lett 32: L22709

Authors' address: A. V. Eliseev (e-mail: eliseev@ifaran.ru, eliseev_av@mail.ru), I. I. Mokhov (e-mail: mokhov@ifaran.ru), A. M. Obukhov Institute of Atmospheric Physics RAS, 3 Pyzhevsky, 119017 Moscow, Russia.